CEBAF Program Advisory Committee Six (PAC6) Proposal Cover Sheet

This proposal must be received by close of business on April 5, 1993 at:

CEBAF
User Liaison Office
12000 Jefferson Avenue
Newport News, VA 23606

Proposal Title

Study of p-n correlations in ^{3}He and ^{4}He with the (e,e'd) reaction

Contact Person

Name: H.P. Blok
Institution: Vrije Universiteit, Dept. of Physics and Astronomy
Address:
Address: De Boelelaan 1081
City, State ZIP/Country: 1081 HV Amsterdam, The Netherlands
Phone: (20) 548 6224 **FAX:** (20) 646 1459
E-Mail → BITnet: **Internet:** HENKB@NAT.VU.NL

If this proposal is based on a previously submitted proposal or letter-of-intent, give the number, title and date:

PR 89-029 Study of the (e,e'd) reaction on ^{3,4}He
Oct. 31, 1989

CEBAF Use Only

Receipt Date: 4/5/93 Log Number Assigned: PR 93-010

By: gp

PROPOSAL FOR CEBAF HALL A, JUNE 1993

Study of p-n correlations in ^{3}He and ^{4}He with the (e,e'd) reaction

The HALL A collaboration

Spokesperson: H. P. Blok (VU/NIKHEF, Amsterdam)

Abstract: The (e,e'd) reaction is an attractive way to investigate proton-neutron correlations in nuclei. We propose to study this reaction on ^{3}He and ^{4}He at high values of the three-momentum transfer q, where some problems in the interpretation of the reaction encountered at low q-values are expected to be reduced. The description of the (e,e'd) process in terms of direct deuteron knockout will be checked with the ^{3}He(e,e'd) reaction, for which exact three-body calculations are performed. The ^{4}He target offers the possibility to study both S=1, T=0 and S=0, T=1 correlations in a dense nuclear system. For both nuclei a separation of in-plane structure functions will be performed in order to enhance the sensitivity to different aspects of the reaction. The experiment will be performed in hall A with the two-spectrometer setup. A high luminosity cryogenic He target will be used.

April 5, 1993

1. Introduction

On the nucleon level the atomic nucleus is described as a system of nucleons interacting via two- (or more) body forces. Except for very light systems one usually introduces a single-particle mean field potential, which is the average of all interactions, plus the residual interaction. The mean-field potential yields the single-particle structure of the nucleus, while the residual interaction gives rise to correlations between nucleons. These play an important role in such processes as α-decay or π-absorption, but they also modify the single-particle structure. The mean-field part of the description of the nucleus, as visible in the single-particle structure of the nucleus, has been investigated in quite some detail by various reactions, especially lately by the (e,e'p) reaction [1], in which the one-hole spectral function is measured. Knowledge about correlations in contrast is scarce. Correlations manifest themselves indirectly through a reduction and spreading of single-particle (hole) strength. Further increased strength of the spectral function at high momenta is expected, an effect that still has to be verified experimentally [2].

Some information on correlations has come from two or more nucleon transfer reactions and knockout reactions. However in many cases the results of such investigations are inconsistent. Most probably this is due to the complicated reaction mechanism, which encompasses multi-step processes, optical-model potentials of composite particles, three-body final states (in knockout reactions), etc.

Knockout reactions induced by high-energy electrons have some distinct advantages. The interaction driving the knockout is known and weak, the incoming and outgoing electron waves can be calculated (almost) exactly and in the final state the projectile (the electron) acts as a spectator. Hence the best direct way to study nucleon-nucleon (NN) correlations in nuclei, where the free NN interaction may be modified by the presence of other nucleons (e.g. through three-body forces), is provided by the (e,e'2N) reaction. Unfortunately, even with high duty-factor beams such experiments, especially in the case of the (e,e'pn) reaction, are not easily performed and the obtainable energy resolution is at best a few MeV, while also the three-body character of the final state poses some problems in the theoretical description of the reaction.

Another way to probe p-n correlations is to use the (e,e'd) reaction. Experimentally the (e,e'd) reaction is similar to the (e,e'p) reaction and it has two strongly interacting particles in the final state only. As will be briefly described in section 2, in a direct knock-out model the q-dependence of the (e,e'd) reaction reflects the (short-range) correlation between the proton and neutron in the target nucleus. An important question, though, is to what extent final-state interaction effects, like (e,e'p)(p,d), which involve a strong-interaction vertex, invalidate a direct knock-out description. However, it should be remarked that also the description of the (e,e'pn) reaction suffers from final-state interaction and other uncertainties, like charge-exchange, Δ contributions etc. An experimental study of such complications by e.g. separating different structure functions is much more difficult in case of the (e,e'2N) reaction than in the case of (e,e'd).

For these reasons it is worthwhile to study the (e,e'd) reaction. This has been done in some detail for relatively low values of q on ^{6}Li, ^{12}C and ^{4}He at NIKHEF. As will be discussed in section 3 some of the results seem contradictory. Since calculations for the mass-3 system indicate that this may (partly) be the result of the low q-values and the kinematics used, we propose to study the (e,e'd) reaction at the much higher values of q attainable at CEBAF on targets of ^{3}He and ^{4}He. The virtue of ^{3}He is that exact three-body calculations of the ^{3}He(e,e'd) reaction can be performed [3,4]. Comparison of experimental data taken under different kinematical conditions to the results of such calculations will allow us to investigate the validity of a direct knockout description of the (e,e'd) reaction. Subsequently we will use this knowledge to study ^{4}He, which is a dense, tightly bound nuclear system, where the effects of correlations will be relatively large. The experimental energy resolution is good enough to separate the ^{2}H final state, which has S=1, T=0, from the breakup continuum, which just above threshold is mainly of S=0, T=1 character, thus enabling a study of spin-singlet correlations (see also section 3). Microscopic calculations for the two-nucleon spectral function of ^{4}He are available [5].
In the remainder of this proposal we will discuss the microscopic description of direct deuteron knockout, the existing data and the proposed experiment, including count rate estimates.

2. Formalism for direct deuteron knockout

In a microscopic description of the (e,e'p) reaction, in which the reaction is described as resulting from the interaction of the electron with separate protons (and neutrons) in the nucleus the T-matrix element for the reaction A(e,e'd)A-2 in DWIA may be written as:

$$T = < \phi_d(\rho)\, \chi_d(R)\, \phi_{A-2} \mid F_p(q) e^{iq\cdot r_p} \mid \phi_A >,$$

where the ϕ's are (internal) wave functions of the indicated nuclei and χ_d is the d-(A-2) relative wave function as given, for instance, by an optical-model wave function. Further $F_p(q)$ represents the proton form factor. For clarity in this formula we have assumed only a charge interaction between the electron and the nucleons in the nucleus and we have neglected other FSI processes than elastic scattering and global absorption. Note further that only the direct term is included, exchange terms being left out as they are small in normal kinematics.
By making an A $\rightarrow$ A-2 expansion an overlap function $\phi(r_1,r_2)$ is obtained. Going over to relative and center of mass coordinates of the p-n pair, the overlap function is written as

$$< A\text{-}2 \mid A > = \Sigma_{S,T,\lambda,\Lambda} [\, \phi_{np}^{\lambda,S,T}(\rho)\, \psi_\Lambda(R)\,]_{J^\pi,T},$$

where for simplicity we have assumed A and A-2 to have spin/parity and isospin $0_+,0$ and J^π,T, respectively. The wave functions ϕ and ψ describe the relative and c.m. motion of the p-n pair with

orbital quantum numbers λ and Λ, while S and T are its spin/isospin quantum numbers. Writing $\mathbf{r_p} = \mathbf{R} + \rho/2$ one finds that T contains the factors

$$F(q) \equiv < \phi_d \mid F_p(q)\, e^{iq.\rho/2} \mid \phi_{np} > \qquad \text{and} \qquad < \chi_d(\mathbf{R}) \mid e^{iq.\mathbf{R}} \mid \psi(\mathbf{R}) >.$$

In analogy to the (e,e'p) case the latter matrix element is seen to yield a (distorted) momentum distribution of the p-n pair relative to the A-2 nucleus, $\psi(\mathbf{R})$ being the corresponding bound-state wave function.

The factor F(q) contains only the internal p-n variable, and its value depends on ϕ_{np}, i.e. on the relative wave function of the p-n pair in the parent nucleus i.e. on the (short-range) correlations between the proton and the neutron. Some simple cases are:

(a) $\phi_{np} = \phi_d$ (extreme cluster model).

In this case $F(q) = F_d(q)$, the form factor for scattering of an electron from a free deuteron, and the cross section for the (e,e'd) reaction as a function of q will follow $\sigma_{ed}(q)$, the free elastic electron-deuteron cross section (quasi-elastic deuteron knockout).

(b) $\phi_{np} = \phi_{d'}$.

Here 'd' means that the quantum numbers S and T are the same as for the deuteron, but the radial wave function, e.g. its extension, may be different. As a result the q-dependence of the cross section will be different from the free σ_{ed} (q).

(c) $\phi_{np} = \phi_{\tilde{d}}$, where $\tilde{d}$ is an S=0, T=1 p-n pair like the just unbound singlet state of the deuteron. (In this case the (e,e'd) reaction is not driven by the longitudinal (charge) part of the electromagnetic current operator, but by its transverse part). This is a rather interesting case as it allows to study S=0, T=1 correlations. In fact one such an example has been studied [6].

Some remarks should be made on the treatment of the final-state interaction. Presently for ^{4}He and heavier nuclei this can be treated only within DWIA, where the outgoing d-(A-2) motion is described by some distorted wave. A process like (e,e'p)(p,d), which is not forbidden, is very hard to include for these nuclei. (It should be mentioned that in the high-energy limit the (e,e'p)(p,d) cross section depends on the same correlated wave function as the direct knockout process [7]). For ^{3}He the situation is different, as exact calculations for the final state are possible, which thus include all possible FSI processes.

3. Existing data.

The (e,e'd) reaction has been studied at Saclay [8], NIKHEF [6, 9-12], and MIT [13]. The most extensive data set was collected at NIKHEF on targets of ^{3}He, ^{6}Li, ^{12}C and ^{4}He. Globally the results can be summarized as follows:

1) The q-dependence of the cross section (after a correction for different FSI effects at the different q) for ^{6}Li(e,e'd)^{4}He is very well described by the free σ_{ed} (q), see fig. 1 (similar results were obtained at Saclay[8]). These results indicate that the reaction can be described as direct deuteron knockout

according to case a) of section 2; indeed the p-n pair in ^{6}Li resembles very much a free deuteron. Thus the $^6\mathrm{Li} \rightarrow \alpha$+d nuclear structure like the shape of the momentum distribution and the α-d cluster probability could be investigated and compared to the results of α-p-n three-body and cluster-model calculations [10].

2) A similar set of data has been collected on ^{3}He [9]. The q-dependence of the ^{3}He(e,e'd) cross sections, measured at p_m=60 MeV/c, can satisfactorily be described in the momentum transfer interval studied: 350<q<450 MeV/c by a microscopic calculation by Laget including single-rescattering FSI and MEC (see fig. 2). Also the deuteron momentum distribution has been measured up to 200 MeV/c at a fixed value of q=380 MeV/c. The data can within 25% be described by the full calculation of Laget. The diagram that represents coupling of the virtual photon to a correlated pn-pair is important to get a good description of the data. It should be mentioned that later calculations including rescattering in all order [3] show that the latter is an important modification, although the basic picture of a direct deuteron knockout process remains.

3) In the ^{12}C(e,e'd) ^{10}B reaction the transition to the 0^+, T=1 state at 1.74 MeV was studied [6]. The pure transverse character of this transition (see fig. 3) and the q-dependence of the cross section indicate that the transition is due to the direct knockout of an S=0, T=1 p-n pair, which through interaction with the virtual photon makes a spin-isospin flip to an S=1, T=0 deuteron (inverse deuteron electro-desintegration; case c) of section 2).

4) Measurements of the ^{4}He(e,e'd) reaction have also been performed at NIKHEF-K [12]. The q-dependence of the measured cross sections, shown in fig. 4, cannot be described by the free electron-deuteron cross section. Results obtained at MIT/Bates for ^{12}C(e,e'd) indicate a similar, even larger, discrepancy at q^2 = 19.5 fm^{-2} [13]. At first glance this is not too surprising as the proton and neutron are expected to be closer together in ^{4}He than in a free deuteron (case b) of section 2). However, a calculation due to Morita [5] using a realistic variational ^{4}He wave function, which includes various types of correlations, yields a slope that is only slightly different from that of $\sigma_{ed}(q)$, as can be seen in fig. 4. Correction for the non-orthogonality of the wave functions in the entrance and exit channels [14] improves the situation slightly, but the discrepancy remains. Also two-body currents are not expected to solve the problem, as the data were taken in dominantly longitudinal kinematics.

This is a puzzling situation. On the one hand the results for ^{6}Li and ^{12}C and to a lesser extent the limited set on ^{3}He indicate that the reaction can be described as a direct knockout process; on the other hand the data on ^{4}He are not described with this assumption. It could well be possible that e.g. an (e,e'p)(p,d) process gives a large contribution to the ^{4}He(e,e'd) cross section, but then it is not clear at all why the effect of this is not visible in ^{6}Li and especially not in ^{12}C. In the latter case there is a priori no reason why an (e,e'p)(p,d) process should lead to a purely transverse cross section.

A possibility that has to be investigated might be the following. The data for the q-dependence in the ^{4}He case were taken in non-parallel kinematics, whereas the other ones were taken in parallel kinematics. Calculations by Van Meijgaard and Tjon [3] for ^{3}He(e,e'p) indicate that in non-parallel kinematics there are relatively large effects of the interference structure function, which are not easily described within DWIA. Furthermore their calculations suggest that all distortion effects are reduced

at higher values of q. This has led us to propose a study of the (e,e'd) reaction on ^{3}He and ^{4}He at the high values of q available at CEBAF. At lower values of q a similar experiment will be performed at NIKHEF [15].

By taking data in different kinematics the contributions of different structure functions can be separated. The results on ^{3}He can then be compared to exact calculations (such calculations are being performed by Tjon et al. and Gloeckle et al.) in order to study the various contributions to the cross section. Using the acquired knowledge on the description of the reaction we will then study both the ^{4}He(e,e'd)^{2}H and the ^{4}He(e,e'd)pn breakup transition, which just above threshold is mainly of S=0, T=1 character. The latter can experimentally be separated due to the good missing energy resolution that can be obtained with the (e,e'd) reaction. (In this context it should be remarked that in practice these two states can not be separated in a ^{4}He(e,e'pn) experiment).

4. The CEBAF experiment

We propose to take data both ^{3}He and ^{4}He for values of q of 0.7, 1.0 and 1.3 GeV/c in (q,ω) constant kinematics at two energies of the incident electron in each case, so that a separation of the $W_L + W_{TT}$, W_T and W_{LT} structure functions can be performed. The lowest q-value was chosen to join smoothly the highest value attainable at NIKHEF (0.5 GeV/c), while the highest value is limited by the count rates. However, the total range is large enough to probe a completely unknown regime in the p-n correlation. The envisaged range in p_m is from 0 to 250 MeV/c, which covers the major part of the momentum distribution. A summary of the kinematics is given in table 1. Values for the beam energy could be chosen (slightly) differently if needed.

Count rates were calculated based on the present design specifications of the Hall A spectrometers: $\Delta\Omega$ = 8 msr and $\Delta p/p$ = 10%. Moreover, it is assumed that a cryogenic He target of 100 mg/cm^2 thickness is available. According to the present ideas [16] such a target should be able to withstand up to 200 μA electron current. For ^{3}He(e,e'd) we have used the measured momentum distribution from ref. 17. For the ^{4}He(e,e'd) cross sections we have used the calculated momentum distribution of Schiavilla [18] scaled down by appropriate factors in order to include the effect of the final-state interaction.

The single rates have also been investigated. Using the QFS code due to Lightbody and O'Connell [19] we found electron rates of 10^4/sec or less, clearly not imposing any limits on our experiment. The single rate in the hadron spectrometer is presumably dominated by the proton singles. Calculations show that these rates do not exceed the 10^5/sec level. Since protons can be separated from deuterons using standard E-dE techniques, the number of random coincidences entering the analysis of our (e,e'd) data will be very low.

A summary of the estimated count rates is given in table 2, while the number of hours requested is summarised in table 1. We have limited ourselves to kinematics in which the count rate exceeds about 40/hr and have tried to collect in each kinematic more than 1000 counts unless this would lead to

prohibitively long measuring times. Especially at the higher q-values we may be able to use a larger target thickness provided the target can stand the high beam current. In fact the constraint on the target thickness for ^{4}He is that the missing-energy resolution remains below 2 MeV. If the luminosity can be increased we can extend the p_m-range at the higher q-values with the same beam time.
According to table 1 the beamtime needed for the actual measurements amounts to about 350 hrs. For target thickness and other calibrations we estimate another 50 hrs, so that the total beam time request is 400 hrs.

References

[1] see e.g. L. Lapikás, 'Quasi-Elastic Electron Scattering off Nuclei', Proceedings International Nuclear Physics Conference, Wiesbaden, July 26 -August 1, 1992
[2] NIKHEF proposal 91-19, spokesperson L. Lapikás
[3] E. van Meijgaard and J.A. Tjon, Phys. Rev. C42 (1990) 74 and 96
[4] W. Gloeckle et al., submitted to Phys. Rev. C
[5] H. Morita et al., Prog. Theor. Phys. 78 (1987) 1117, ibidem 79 (1988) 863 and H. Morita, private communication
[6] R. Ent et al., Phys. Rev. Lett. 62 (1989) 24
[7] G.R. Satchler, Direct nuclear reactions, Oxford University Press, 1983
[8] M. Jodice et al., Phys. Lett. 282 (1992) 31
[9] P.H.M. Keizer et al., Phys. Lett. 157B (1985) 255
[10] R. Ent et al., Phys. Rev. Lett. 57 (1986) 2367
[11] R. Ent, Ph. D. Thesis, Vrije Universiteit Amsterdam (1989)
[12] R. Ent et al., Phys. Rev. Lett. 67 (1991) 18
[13] L. B. Weinstein and W. Bertozzi, Proceedings of the fourth workshop on Perspectives in Nuclear Physics at Intermediate Energies, 8 - 12 May 1989, Trieste, Italy
[14] W. Leidemann et al., Phys. Lett. 279 (1992) 212
[15] NIKHEF proposal 91-07, spokesperson H.P. Blok
[16] Report to Technical Advisory Panel for the High Resolution Spectrometer, TAP2 (HRS), June 28-30, 1989, CEBAF, Newport News
[17] E. Jans et al., Nucl. Phys. A475 (1987) 687
[18] R. Schiavilla, V. R. Pandharipande and R. B. Wiringa, Nucl. Phys. A449 (1986) 219
[19] J.W. Lightbody and J. S. O' Connell, Computers in Physics, 1 (1988) 57

Table 1 Kinematics for the ^{3,4}He(e,e'd) reaction

q [GeV/c]	E [GeV]	$\theta_{e'}$	E	$\theta_d(p_m=0)$	p_m-range [MeV/c]	hrs ^{3}He	hrs ^{4}He
0.7	1.5	27.8	0.89	-64.1	-250(50)250	31	17
	0.55	93.6	0.30	-34.7	-150(50)150	29	30
1.0	2.2	27.0	0.89	-61.0	-150(50)150	17	15
	0.8	95.7	0.28	-31.6	-100(50)100	38	60
1.3	3.0	25.5	0.90	-58.4	-100(50)100	21	52
	1.1	91.2	0.30	-35.6	0 only	8	16

Table 2 Estimated count rates per hour for ^{3}He/^{4}He

q [GeV/c]	E [GeV]	p_m=0	50	100	150	200	250
0.7	1.5	72000/13000	27000/9000	7000/4500	1300/2200	270/900	60/270
	0.55	4400/800	1650/550	440/275	80/140		
1.0	2.2	9000/1650	3300/1100	900/550	165/275		
	0.8	400/75	150/50	40/25			
1.3	3.0	1000/200	400/130	100/65			
	1.1	40/7.5					

Figure Captions

Fig. 1. The cross section for the reaction ^{6}Li(e,e'd) as a function of the momentum transfer, compared to the quasi-elastic electron-deuteron cross section.

Fig. 2. The cross section for the reaction ^{3}He(e,e'd) as a function of the momentum transfer, compared to different calculations.

Fig. 3. Longitudinal-transverse separation for the ^{12}C(e,e'd)^{10}B$_{1.74MeV}$ transition.

Fig. 4. The cross section for the reaction ^{4}He(e,e'd) as a function of the momentum transfer, compared to a quasi-elastic and a full microscopic calculation.

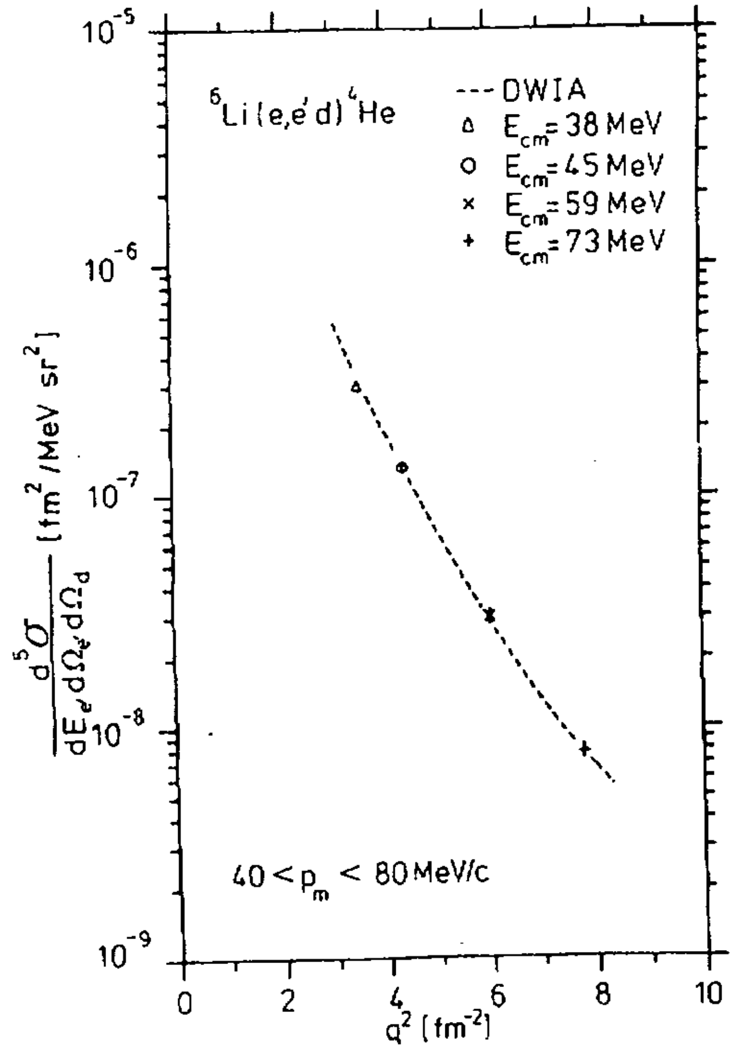
$\frac{d^5\sigma}{dE_{e'}d\Omega_{e'}d\Omega_d}$ [fm^2/MeV sr^2]
10^{-5}
10^{-6}
10^{-7}
10^{-8}
10^{-9}
^{6}Li(e,e'd)^{4}He
--- DWIA
Δ E_{cm}= 38 MeV
o E_{cm}= 45 MeV
× E_{cm}= 59 MeV
+ E_{cm}= 73 MeV
40 < p_m < 80 MeV/c
0
2
4
6
8
10
q^2 [fm^{-2}]

Fig. 1

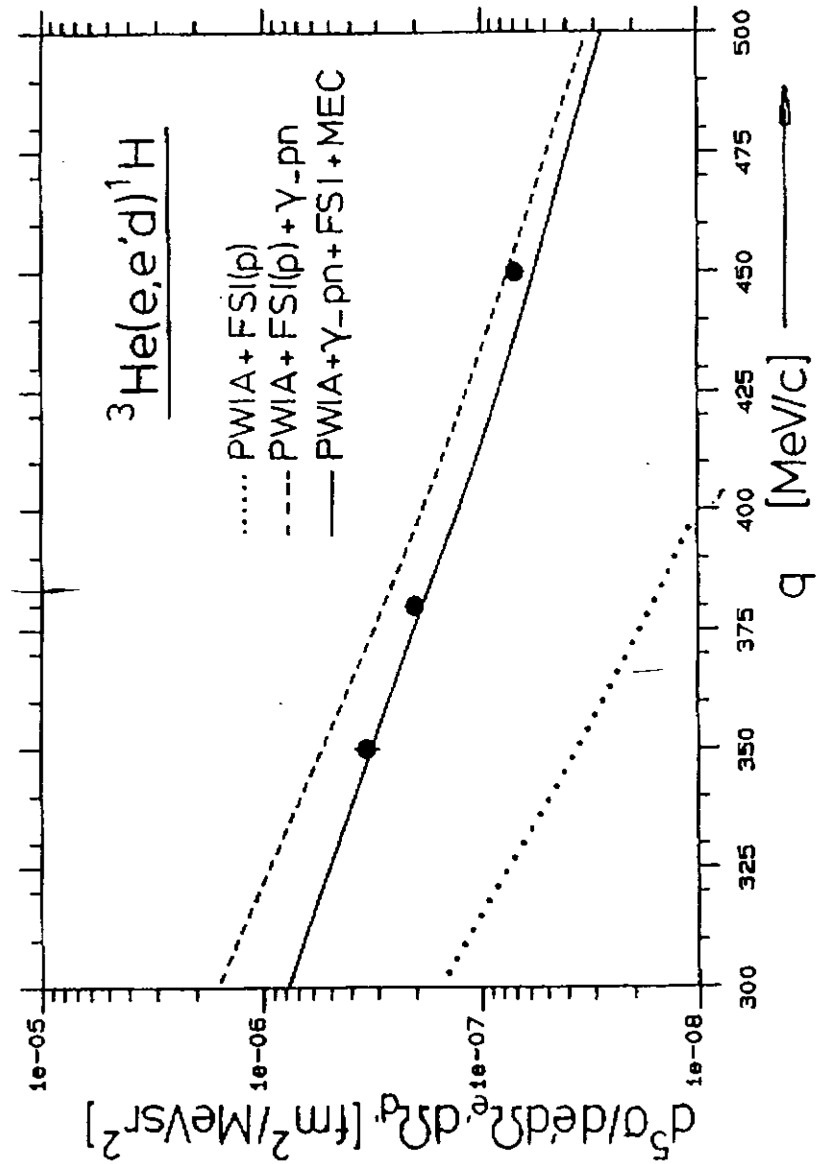
^{3}He(e,e'd)^{1}H
PWIA + FSI(p)
PWIA + FSI(p) + γ_pn
PWIA + γ_pn + FSI + MEC
$d^5\sigma/de'd\Omega_{e'}d\Omega_{d'}$ [fm^2/MeVsr^2]
1e-05
1e-06
1e-07
1e-08
300
325
350
375
400
425
450
475
500
q [MeV/c]

Fig. 2

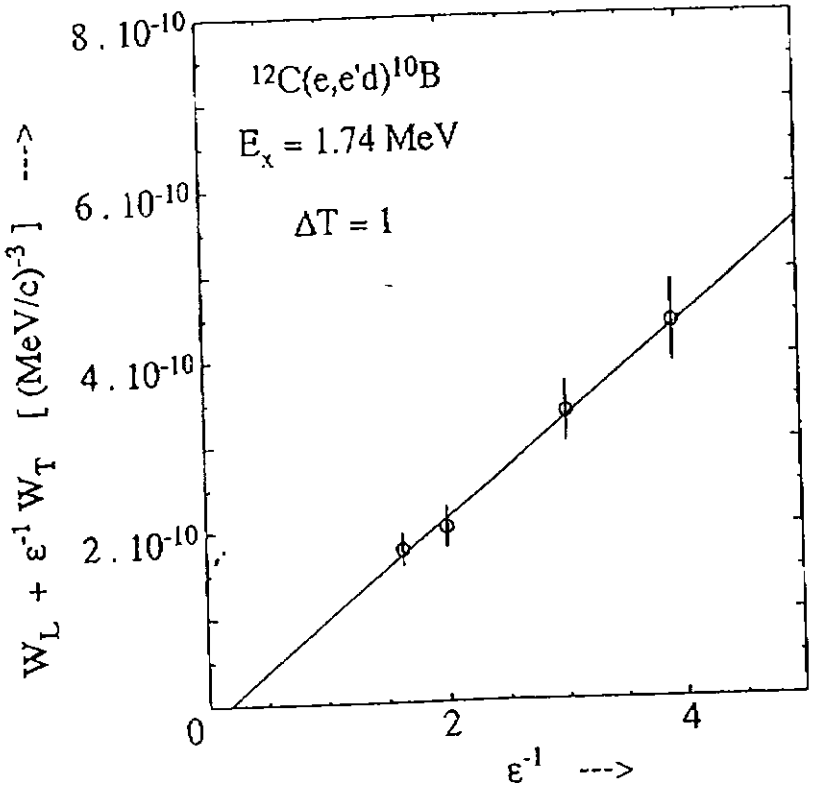
$^{12}C(e,e'd)^{10}B$
E_x = 1.74 MeV
$\Delta T = 1$
$W_L + \varepsilon^{-1} W_T$ [(MeV/c)$^{-3}$] --->
ε^{-1} --->
8 . 10^{-10}
6 . 10^{-10}
4 . 10^{-10}
2 . 10^{-10}
0
2
4

Fig. 3

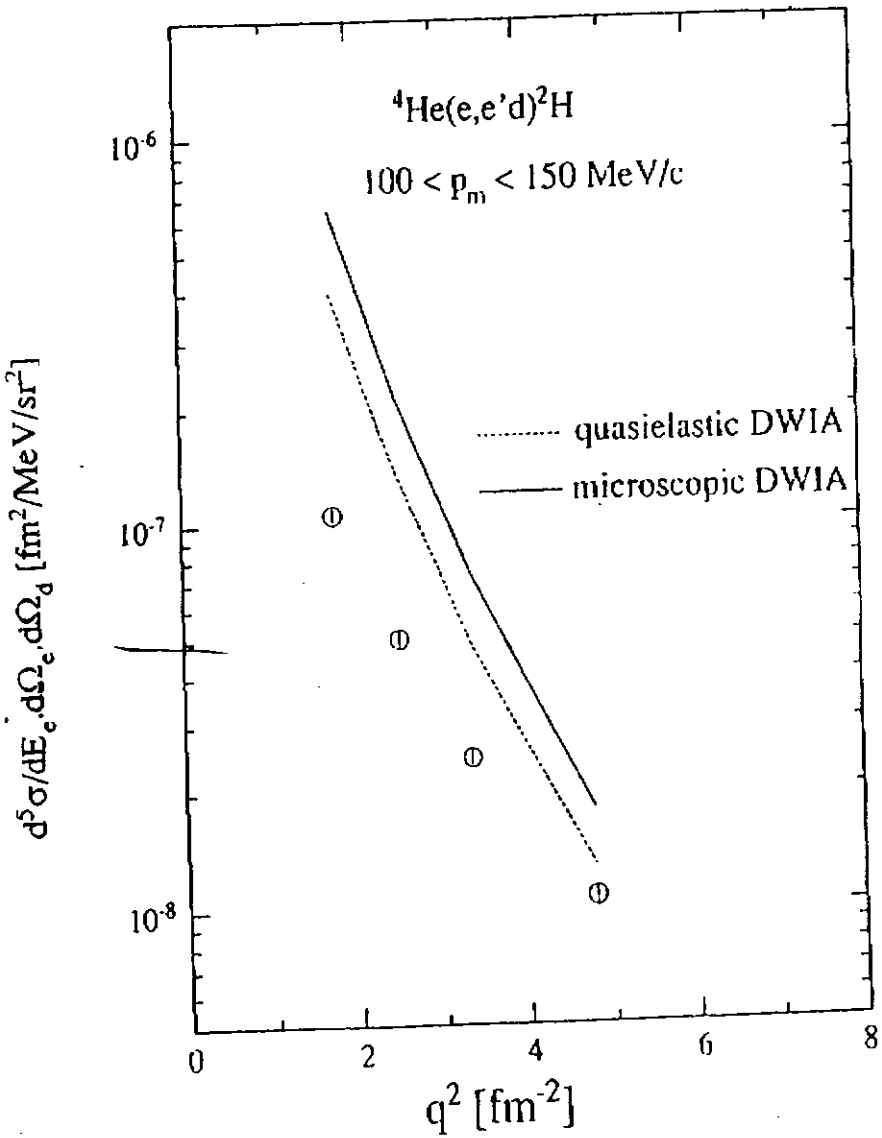
$^4He(e,e'd)^2H$
$100 < p_m < 150$ MeV/c
quasielastic DWIA
microscopic DWIA
$d^5\sigma/dE_e'.d\Omega_e.d\Omega_d$ [fm^2/MeV/sr^2]
q^2 [fm^{-2}]
10^{-6}
10^{-7}
10^{-8}
0
2
4
6
8

Fig. 4

same momentum being detected. The lower initial momenta are more sensitive to MEC and FSI, while the higher are sensitive to correlations. Combined measurements in anti-parallel and symmetric configurations and theoretical input are thus needed to unfold the various mechanisms.

Using Laget's code [39], cross sections were calculated for various electron beam energies and electron scattering angles, resulting in a range of energy and momentum transfer, and initial proton momenta in the cm-system.

The high energy nucleons will be detected in HARP, which will be placed at forward angles. This is done in order that the somewhat higher threshold of HARP (60 MeV for neutrons and 100 MeV for protons) does not hamper the choice of kinematics. For those kinematics in which the nucleons have kinetic energies exceeding 800 MeV, we have the option to use the hadron (HRSH) spetrometer, if the efficiency of HARP decreases too much. For all other cases, the HRSH will be placed at backward angles and will detect low energy protons.

HARP has an efficiency of 3 %. This is not a hindrance for neutron detection, since the np-channel has large cross sections. This efficiency applies as well to protons, and its adverse effect is mostly negated by operating at a high luminosity. The use of a dedicated proton detector such as the Hadron-IV device (developed and built by the Vrij Universiteit and NIKHEF-K in the Netherlands), is being evaluated as a possible substitute for HARP, in connection to some pp-measurements. Hadron-IV has a nominal solid angle of 500 msr, but it would be employed at a large distance from the target, in order to cope with the high luminosity, thus reducing the effective solid angle to the order of 5 msr. The use of Hadron-IV depends on its performance in a high luminosity environment, which will be established in the coming two years at AmPS.

The chosen kinematics, cross sections and count rates are shown in table 1 below, where the five-fold differential cross section is expressed in $pb/(MeV/c)^2/sr^3$. The momentum acceptance of the electron and proton spectrometers was taken to be $\Delta p/p = 10$ %, the luminosity was 2.25×10^{38} $cm^{-2}s^{-1}$, and the detector solid angles were [42]: $\Delta\Omega_e(8°) = 4.9$ msr, $\Delta\Omega_e(15°) = 7.9$ msr, $\Delta\Omega_{p_1} = 16.0$ msr and $\Delta\Omega_{HARP} = 50$ msr. The luminosity of 2.25×10^{38} $cm^{-2}s^{-1}$ corresponds to a beam current of 150 μA on a high pressure ^{3}He gas target of density 1.20 g/cm^2.

3.1.2 Anti-parallel Kinematics

Following the absorption of the photon the two protons are ejected back to back (180° apart) in the laboratory. This geometry has the advantage of minimizing final state interactions between the ejected protons, since they leave in opposite directions. This is the geometry in which the L/T separation will be carried out, since only the longitudinal and the transverse response functions contribute to the cross section. The longitudinal component is the most sensitive indicator of correlations. An initial set of these kinematics are shown in table 2, which is being refined with the aid of theoretical calculations, since their requirements are stringent and difficult to

Table 1: Count Rate Estimates for Symmetric Kinematics

E_e GeV	ω MeV	q MeV/c	θ_e	p_i MeV/c	T_i MeV	θ_1	θ_2	$d^5\sigma$	rate hr^{-1}
2	200	565	16	436	96	-11.9	-111.1	0.0763	3022
2	300	375	7	544	146	36.3	-103.4	4.0953	120195
4	400	1068	15	638	196	-27.6	-93.8	0.0123	1429
4	500	1097	15	723	246	-15.0	-96.3	0.0099	1267
4	600	1189	16	802	296	-9.9	-94.2	0.0080	1100
4	700	829	7	877	346	32.8	-90.8	0.1660	15257
4	800	912	7	949	396	36.0	-86.6	0.0698	6732

Table 2: Anti-Parallel Kinematics

E_e GeV	ω MeV	q MeV/c	θ_e	ϵ	θ_{cm}	p_1 MeV/c	θ_1	p_2 MeV/c
3.0	900	1076	13	0.91	0	1475.97	-27.10	399.80
3.0					180	399.80	152.90	1475.97
1.3			46	0.44	0	1475.80	-16.48	400.18
1.3					180	400.18	163.52	1475.80
3.5	1200	1348	12	0.90	0	1798.16	-21.55	450.05
3.5					180	450.05	159.46	1798.16
1.9			30	0.58	0	1798.18	-15.46	450.01
1.9					180	450.01	164.54	1798.18

accomplish.

The cross sections for these kinematics were obtained in two ways. For the forward angle of each point, where the longitudinal component dominates, Laget's code was used. At the large electron angle, real photon data [9, 40] was suitably manipulated to effectively yield the transverse component of the reaction in question. This involved using the mass dependent empirical formula for estimating the (γ, p) cross sections together with the $^9Be(\gamma, pn)$ and $^9Be(\gamma, pp)$ angular correlation data [40]. The resulting figures were checked against the $^3He(\gamma, p)$ results from reference [9] and were found to be in agreement.

3.2 The ^{3}He(e, e'np) Reaction

It is well known from pion and real photon absorption experiments, that the (e, e'np) cross sections are about 10 to 20 times larger than the corresponding cross sections of the pp-channel. The PW calculations of Laget and Tjon indicate precisely the

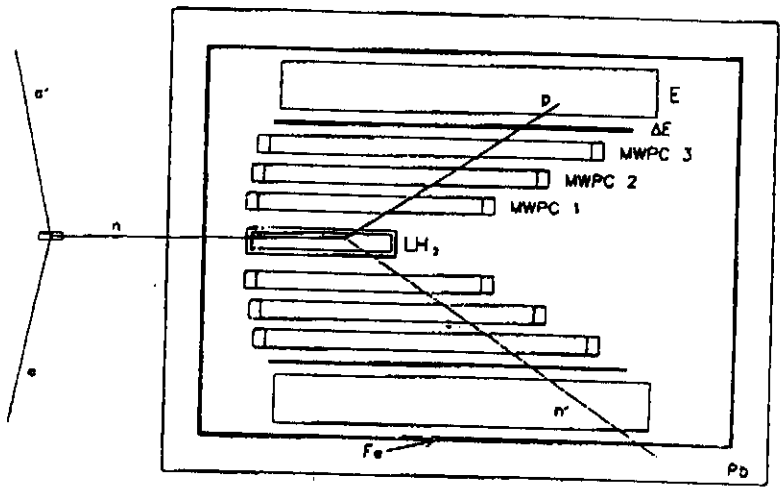

Figure 15: A schematic representation of the geometry for HARP.

same fact, and the two codes agree to a level of 10 % on the np/pp ratio. Hence, since protons and neutrons will be detected simultaneously, the desired statistical precision is defined by the pp-channel.

3.3 Singles and Accidental Coincidence Rates

Detailed calculations of the singles and accidental counting rates involving HARP and the HRS[2] spectrometers are in progress. A Monte Carlo physics event generator (ENIGMA [41]) feeds the GEANT detector simulation package. No background problems are anticipated due to the triple-coincidence between these three devices and the inherent low-noise of HARP (which employs at least a four-fold internal coincidence).

3.4 The HARP Neutron Polarimeter

3.4.1 Principle of Operation

HARP operates on the recoil principle. Its design is based on $\Delta E - \Delta E - E$ scintillator detector telescopes and tracking devices (Multi Wire Proportional Chambers, MWPC) placed around the converter, which contains liquid hydrogen (LH_2). Eight such telescopes and three MWPCs will be positioned at either side of the converter (see Figures 15 and 16).

HARP can be used for protons as well, since they also scatter in the converter, and both scattered and recoil protons can be subsequently detected. HARP can detect both incoming protons and neutrons simultaneously by employing an "intelligent" trigger, and a charged particle tagger between the target and the converter.

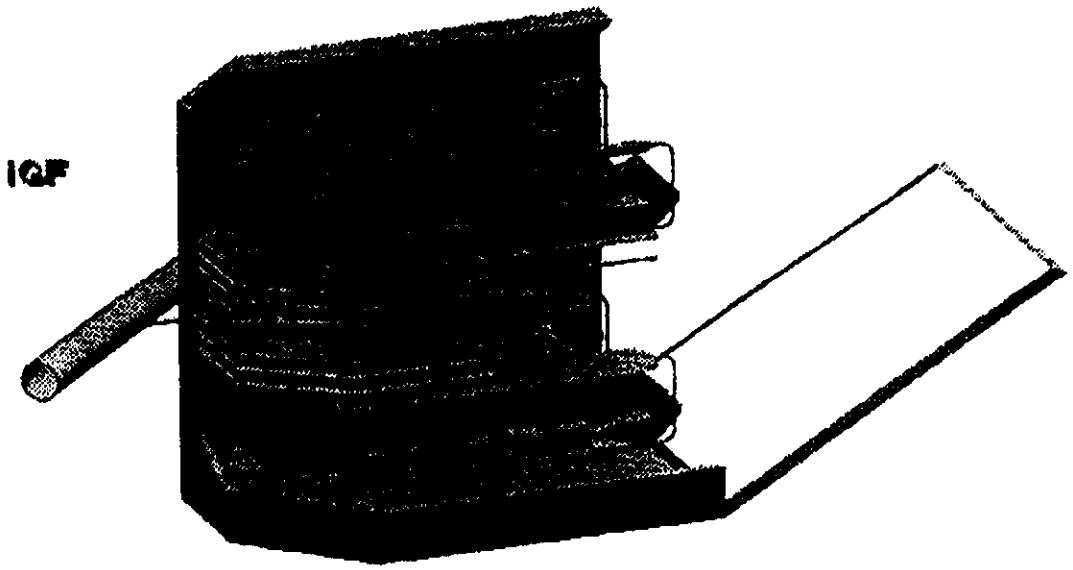

Figure 16: A three-dimensional representation of HARP. Also visible is the beam pipe (slanted cylinder) and the drop-down rear wall of surrounding shielding house).

Selected results of the simulations serve to illustrate the expected performance of HARP [43]. The efficiency is approximately 3 %, and remains roughly constant as a function of the nucleon kinetic energy. The energy resolution ($\Delta T_n/T_n$) is modest (8 %), but it also remains relatively constant up to 800 MeV nucleon energy. Simulations are underway to determine whether these properties change significantly in the range from 800 to 1200 MeV. These characteristics are coupled to a very high insensitivity to background, and hence the tolerance of a very high luminosity.

3.4.2 The Design of HARP

The design of HARP is described in detail elsewhere [44]. A trapezoidal shape has been chosen for the LH_2 converter, of 3 cm height and 60 cm depth (along the path of the neutron). The front and rear sides are 80 cm wide and 150 cm wide, respectively, yielding a large surface area. This sheet will contain about 25 liters of LH_2. A prototype vessel is under construction at NIKHEF-K and will be soon tested together with the cryo-system.

The HARP detectors can be setup in two orientations: the scintillator walls being horizontal (U-D configuration), or vertical (L-R). The former will be employed in this experiment since it offers the maximum solid angle of HARP, 50 msr. In this configuration the minimum angle with respect to the beamline which can be reached is 45°. For this angle, HARP can simultaneously measure particles from 15° to 75°.

The E-counters will have a thickness of 20 cm, and can thus stop up to 175 MeV perpendicularly impinging protons. The two ΔE detectors are 3 mm and 10 mm thick, respectively. The ΔE layers allow for a secure proton identification down to 18 MeV, and "tighten" the trigger level for proton energies beyond 40 MeV. A

charged particle tagger will be positioned in front of the converter, to discriminate between incoming protons and neutrons, and will consist of two overlapping planes of narrow plastic scintillator strips equipped with small photomultiplier tubes.

The detectors will be enclosed in a 6 cm thick lead-steel house to be shielded from background. The total weight for HARP is estimated at 25 tons which includes a platform to allow for rotation around the target center-post.

3.4.3 The Merits of HARP

The recoil principle leads to a large background suppression by eliminating photons and low energy neutrons, and it permits recoil detectors to operate at much higher luminosities than TOF detectors. This is partly a result of shielding the sensitive detectors: they do not "look" directly at the target (which is also a source of unwanted background events) but are placed behind walls. In addition, the high-fold coincidence required to detect the proton (four wire chamber planes and two scintillators) further reduces the neutral background. Finally, measurements of the energy and time variables of the detected particles are carried out independently. In this manner, the two variables may be used to cross check each other, effectively compressing the neutron TOF spectrum into a narrow peak, hence improving the S/N ratio. HARP will thus operate at a much higher luminosity than other n-detector system. This reduces the experimental beam time needed in order to obtain the required statistical precision, or conversely allows the measurement of processes with much lower cross sections.

A final advantage of HARP is that it is relatively easy to calibrate with respect to the efficiency of detection and of n-p conversion. This procedure involves the determination of the wire chamber efficiency in a pairwise cyclic manner, while the scintillators may be calibrated in situ with a reaction of known kinematics and cross section (e.g. via ^{1}H(e,e'p) with the protons detected in HARP). The PMT gain will be continuously monitored with a flasher ADC/fiber optic system, coupled to a counter which is continuously referenced to an ^{241}Am source.

HARP will be commissioned at AmPS using an unpolarized electron beam in mid-1994. Measurements on ^{1,2}H targets will be performed, in which the electron elastically scatters from the proton and respectively the neutron, and both the scattered electron and the nucleon are detected. These measurements will serve to get the instrument fully operational and will provide a check of the calibration procedure. The device will be shipped to Hall-A as dictated by the physics interest of the HARP and Hall-A collaborations and depending on the experimental scheduling.

3.5 The Primary Target

Targets for this experiment and related experiments are being currently designed and constructed. These designs call for cryogenic gas targets to be operated at a high pressure. The design addresses the issues of the required high density to achieve

Table 3: Beam Time Estimate for Symmetric Kinematics

E_e GeV	ω MeV	q MeV/c	rate hr^{-1}	HRSH bins	HARP bins	Time hours
2	200	565	3022	2	5	110
2	300	375	120195	2	5	3
4	400	1068	1429	2	5	230
4	500	1097	1267	2	5	260
4	600	1189	1100	2	5	300
4	700	829	15257	2	5	20
4	800	912	6732	2	5	50
					Counting time	973

luminosities of 10^{38} $cm^{-2}s^{-1}$, the large amounts of heat deposited by the beam in the target, the high energy densities at the interaction region due to the small size of the beam spot, the containment of density flucutations due to beam heating and minimizing the thickness of the target cell windows.

A preliminary design for a ^{3}He cell specifies a minimum operating temperature of 10 K and pressure of 70 atm. The corresponding target gas density is 80 mg/cm^3. For an effective cell length of 15 cm (perpendicular), luminosities of 10^{38} can be achieved for beam currents of 50-150 μA. For a cylindrical cell of 15 cm (physical) length with spherical end caps, a wall thickness of 0.03 cm of aluminum 7075-T6 is being incorporated in the current design. This design specifies that the target cell be viewable by two spectrometers simultaneously (one on each side of the beam pipe), over an angular range of $10^o - 130^o$ in the scattering plane and $\pm 10^o$ out of plane. The latter figure is more than sufficient as far as HARP is concerned, since this device will have a $\pm 3^o$ out of plane acceptance in its U-D configuration.

The bulk power dissipation in the target will be dealt with a L^{4}He refrigerator and a suitable heat exchanger. For the ^{3}He target cell, a maximum power dissipation of 1.0 kW (for a 200 μA beam) is anticipated. To minimize density variations due to local beam heating, it is necessary that the target gas flows past the beam. Current preliminary designs specify a gas flow perpendicular to the beam direction, at velocities as high as 30 m/s, assuming a tolerable density variation of no more than 20 % for a minimum beam spot size of 0.1 mm. Experience in other laboratories, e.g. SLAC, indicates that such velocities can indeed be realized. For a 10 % density variation, these velocities must be roughly doubled, though they can be reduced substantially (by more than a factor of two) if the beam is defocused or rastered. For example, it appears that it will be possible for the beam to be defocused to 1-2 mm (horizontally) which reduces the flow velocities by at least a factor of five.

The group from California State University is involved in the design of these targets, in consultation with John Mark, a target specialist at SLAC.

Table 4: Beam Time Estimate for Anti-Parallel Kinematics

E_e GeV	ω MeV	q MeV/c	ϵ	rate hr^{-1}	HRSH bins	HARP bins	Time hours
3.0	900	1076	0.91	104	4	10	171
1.3			0.44	100	4	10	178
3.5	1200	1348	0.90	103	4	10	172
1.9			0.58	141	4	10	126
						Counting time	647

Table 5: Total Beam Time Estimate

	hours
Symmetric kinematics	973
Anti-Parallel kinematics (L/T)	647
Setup, calibration, angle changes	300
Total time	1920

3.6 Beam Time Estimate

We wish to observe the complete proton spectrum for each 10 % byte in the electron momentum of the HRSE spectrometer. Assuming 100 MeV/c bytes for the symmetric case, the momentum range in the proton spectrometer can be covered in 2 bins. In the L/T case (anti-parallel) a finer binning was taken to reflect the higher accuracy desired in these measurements. HARP was binned in a similar manner. Assuming a desired 1000 counts/bin, we arrive at the counting times shown in tables 3 and 4. According to these calculations the amount of running time is 1620 hours. Adding 300 hours for setup time, testing, angle and energy changes, and contingency brings the total beam time request to 1920 hours (table 5). These numbers have been calculated assuming operation at a luminosity of $2.25 \times 10^{38}\,cm^{-2}s^{-1}$ and a 3 % efficiency for HARP.

4 Acknowledgements

We wish to thank M.J. Dekker for his comments on the proposal and useful discussions on theoretical aspects of the proposal.

References

[1] S. Auffret et al., Phys. Rev. Lett. **55** (1985) 1362.

[2] G. van der Steenhoven et al., Nucl. Phys. **A480** (1988) 547.
J.B.J.M. Lanen et al., Phys. Rev. Lett. **64** (1990) 2250.

[3] P.E. Ulmer et al., Phys. Rev. Lett. **61** (1988) 2001.
P.E. Ulmer et al., Phys. Rev. Lett. **59** (1987) 2259.

[4] Z-E. Meziani et al., Phys. Rev. Lett. **54** (1985) 1233;
Z-E. Meziani et al., Phys. Rev. Lett. **52** (1984) 2130.

[5] C. Marchand et al., Phys. Rev. Lett. **60** (1988) 1703.

[6] J. Ahrens et al., Phys. Lett. **146B** (1984) 303.

[7] P. Carlos et al., Nucl. Phys. **A431** (1984) 573.

[8] T. Emura et al., The TAGX collaboration, Phys. Rev. Lett. (submitted).

[9] G. Adams et al., The LEGS collaboration, private communication (1993).

[10] P. Weber et al., Phys. Rev. **C43** (1991) 1553.

[11] P. Weber et al., Nucl. Phys. **A534** (1991) 541.

[12] J.D. Silk, Phys. Rev. **C37** (1988) 891.

[13] H. Baghaei et al., Phys. Rev. **C39** (1989) 177.

[14] R.D. McKeown et al., Phys. Rev. Lett. **44** (1980) 1033.

[15] Th.S. Bauer, Invited talk at the International Workshop with BLAST, Tempe, Arizona, March 1992 to be published.
A. Zondervan, Ph.D. Thesis, University of Amsterdam, unpublished (1992).

[16] M.J. Dekker et al., Phys. Lett. **289B** (1992) 255.

[17] R.W. Lourie et al., Phys. Rev. Lett. **56** (1986) 2364.

[18] T. Takaki, Phys. Rev. Lett. **62** (1989) 395.

[19] H. Primakoff and T. Holstein, Phys. Rev. **55** (1939) 1218.

[20] J.M. Laget, Phys. Rev. **C38** (1988) 2993;
J.M. Laget , J.Phys. G: Nucl. Phys. **14** (1988) 1445 .

[21] S. Coon and B. Friar, Phys. Rev. **C34** (1986) 1061.

[22] A.J. Sarty, Nucl. Phys. **A543** (1992) 49;
N.R. Kolb et al., Western Regional Nuclear Conference, Lake Louise, February 1993 (unpublished).

[23] G. Audit et al., Phys. Rev. **C44** (1991) R575.

[24] H. Arenhovel and M. Sanzone, Few Body Systems Suppl. 3, Springer Verlag, Wien, N.Y.

[25] G.E. Brown et al., Phys. Lett. **118B** (1982) 39;
B. Schwesinger et al., Phys. Lett. **132B** (1983) 269.

[26] E. Oset et al., Nucl. Phys. **A448** (1986) 597;
M.J.V. Vacas and E. Oset, private communication (1993);
L.L. Salcedo et al., Nucl. Phys. **A448** (1988) 557.

[27] S. Barshay and D. Rein, Zeit. fur Phys. **C46** (1990) 215; S. Barshay, Mod. Phys. Lett. **A5** (1990) 107.

[28] W. Kratschmer, Nucl. Phys. **A298** (1978) 477.

[29] S. Boffi, Proceedings of the Topical Workshop on Two-nucleon Emission, ed. O. Benhar and A. Fabrocini (ETS editrice, Pisa, 1991) 87.

[30] G. Orlandini and W. Leidermann, private communication.

[31] C. Giusti et al., Nucl. Phys. **A546** (1992) 607.

[32] C. Giusti and F.D. Pacati, Nucl. Phys. **A535** (1991) 573.

[33] H. Yokota et al., Phys. Rev. Lett. **58** (1987) 191.

[34] Z. Papandreou et al., Phys. Lett. **227B** (1989) 25.

[35] G.J. Lolos, TRIUMF experiment E555 (1989).

[36] C.L. Morris and R.D. Ransome, "Pion Absorption on Light Nuclei", LAMPF Progress Report LA-12256-PR (1990) 17.

[37] E. van Meijgaard and J.A. Tjon, Phys. Rev. **45** (1992) 1463.

[38] S. Boffi and M.M. Giannini, Nucl. Phys. **A533** (1991) 441.

[39] J.M. Laget, Phys. Rev. **C35** (1987) 832.

[40] M. Kanazawa et al., Phys. Rev. **C35** (1987) 1828.

[41] J.L. Visschers, ENIGMA Monte Carlo, version 2.4, unpublished (1993).

[42] J. Le Rose, CEBAF, private communication (1989).

[43] H.W. Willering, "Optimization of the HARP Detector", Utrecht Internal Report V(SAP) 92-14, October 1992.

[44] Z. Papandreou et al., "High Acceptance Recoil Polarimeter", CDR v2.0, Utrecht University Internal Report, August 1992.